




A Procedure for Validating Impedance Parameters of HF/UHF RFID Transponder Antennas

Piotr Jankowski-Mihułowicz¹ , Mariusz Węglarski¹,
and Wojciech Lichon²

¹ Department of Electronic and Telecommunications Systems,
Rzeszow University of Technology, Pola 2, 35-959 Rzeszow, Poland
{pjanko, wmar}@prz.edu.pl

² Talkin Things, Pulawska 182, 02-670 Warsaw, Poland
wojciech.lichon@talkinthings.com

Abstract. The performance of automatic identification in every RFID system is strongly dependent on proper operation of the transponders that are used to mark different kind of objects. The impedance matching between chip and connected antenna is the most significant component determining the design quality of transponder internal circuitry, and hence influencing overall system parameters such as shape and dimensions of interrogation zone, level of identification efficiency, etc. Taking into consideration the various types of RFID systems, the problem has to be considered differently with respect to the operating frequency. Moreover it has to be treated in a different way than it is known from the classical theory of typical radio communication systems. The authors have proposed and developed their own method for validating impedance parameters of RFID transponder antennas operating in the regular HF and UHF bands. It is based on a generalized model of the RFID transponders dedicated to different standards. The developed test procedure consists of four steps involving antenna designing, manufacturing, measuring and validating processes. The practical usefulness of the proposed method is confirmed by experiments conducted with using representative examples designed in research and development projects realized with partners from the industry.

Keywords: RFID · HF · UHF · Transponder · Antenna · Impedance Validation

1 Introduction

Progress in the electronics, telecommunications, computer science, robotics and control engineering as well as in many other areas of the technology has a significant impact on changes in the human environment [1]. As a consequence of these alternations, the growing number of intelligent technology implementations with ability to support an advanced automatic identification of objects is observed [2, 3]. The radio frequency identification (RFID) technology is commonly used in such systems [4–6].

The RFID systems are placed in a group of radio equipment devices [7]. They use bands (LF, HF, UHF, etc.) and operating frequencies that are commonly available for industrial-scientific-medical (ISM) and many other purposes [8]. Therefore, the band and operating frequency constitute basic factors influencing the differentiation between types of RFID systems. They subsequently determine a different approach in terms of considering the performance essence of the systems.

Irrespective of the mentioned frequency bands, a software and hardware parts may be distinguished in any RFID system. The software serves for both direct control of individual digital devices as well as for managing the whole system. The hardware part is composed of a read/write device (RWD) with at least one antenna and a single or many electronic transponders which are used to mark objects.

The RFID transponder consists of a chip with a connected antenna [7]. The impedance matching of these two components is the basic requirement for the proper operation of this electronic device. This problem has to be considered differently with respect to constructions that are commonly used in RFID systems operating in HF [9–11], UHF [12–18] or multi bands [19]. It should be emphasized that the efficiency of automatic identification of electronically marked objects is determined by the proper operation of the transponders – the design quality of transponder internal circuitry has significant impact on parameters of RFID systems, such as shape and dimensions of interrogation zone (IZ), satisfactory level of identification efficiency, etc. [20].

It should be also noted that phenomenon of impedance matching between the transponder antenna and chip has to be considered in a different way than it is in the classical theory of typical radio communication systems. First of all, the impedance of the chip is represented by two parts: imagine and real, and it differs from the pure real value of 50Ω or 75Ω that is commonly considered in classical radio devices. Moreover, this impedance varies with the amount of power that is transferred from the antenna to the chip. Secondly, the complex impedance of the antenna is vulnerable to the environmental conditions such as kind of material which the marked object is made of [11, 16–18], fluctuations of ambient temperature [21] and many others. Thirdly, connectors (N, SMA, UFL, etc.) are not applicable to the components of the transponder and, on the other hand, the type of interconnection structure in the chip has significant impact on the impedance of the antenna [22] and methods that are used to measure this parameter [23]. Finally, the antenna design determines the selection of measuring equipment.

The method for validating impedance parameters of RFID transponder antennas operating in the regular HF and UHF bands has been developed taking into consideration the above mentioned conditions. It has been worked out on the basis of the authors' experience that had been growing and expanding for several years during numerous projects related to industrial implementations of RFID devices. The proposed method can be adapted to both scientific as well as industrial research and development laboratories. Since it arises from the generalized model of the RFID transponder (Sect. 2), the impedance parameters of the device can be validated on the basis of algorithm yielded from the model synthesis (Sect. 3). The practical usefulness of the developed method is confirmed on the basis of a few representative examples (Sect. 4), which are the result of the research and development cooperation between the Department of Electronic and Telecommunications Systems (DETS) in Rzeszow University of Technology (RUT) and industry partners.

2 Impedance Model of HF/UHF RFID Transponder

Internal constructions as well as operation principles of transponders are strongly dependent on the considered frequency band and the carrier frequency (in the HF band f_0 is equal 13.56 MHz, in the UHF band: $f_0 = 860\text{--}960$ MHz depending on world regions). Nevertheless, the generalized model is proposed for the desired measuring process that could be used for validating required parameters in any RFID system (Fig. 1).

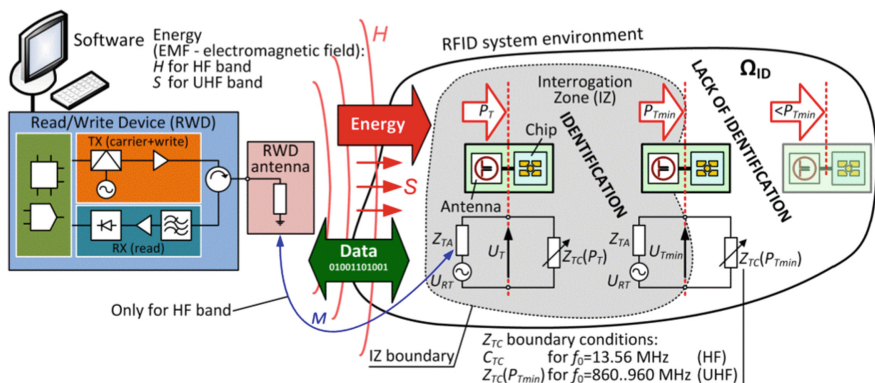


Fig. 1. Impedance model of HF/UHF RFID transponder in RFID system

In the model, transponder blocks are respectively represented by impedance of the antenna (Z_{TA}) and the chip (Z_{TC}). The impedance Z_{TA} has an inductive nature and is constant for a given operation frequency of a transponder. In the serial equivalent, it can be written as:

$$Z_{TA} = R_{TA} + jX_{TA} = R_{TA} + j\omega L_{TA} \quad (1)$$

where: R_{TA} denotes the resistance of a transponder antenna, X_{TA} – reactance which can be expressed by the inductance L_{TA} , $\omega = 2\pi f_0$ describes pulsation.

On the other hand, the chip impedance has a capacitive character and it varies with parameters of the electromagnetic field (EMF). In the serial equivalent, it can be described by the following dependence:

$$Z_{TC} = R_{TC} + jX_{TC} = R_{TC} + \frac{1}{j\omega C_{TC}} \quad (2)$$

where: R_{TC} denotes the resistance of an active chip, X_{TC} – reactance which can be expressed by the chip capacitance C_{TC} .

The HF RFID systems operate in the space Ω_{ID} that is characterized by an inhomogeneous magnetic field (expressed by the magnetic field strength H) and strong coupling (expressed by the mutual inductance M) between RWD and transponder antennas. The inhomogeneous magnetic field generated in the RWD antenna vicinity is a medium for both energy transfer and wireless communications. The minimum

magnetic field strength H_{min} at which the correct data transmission between the RWD and transponder takes place is an EMF boundary condition that characterizes the interrogation zone and read/write range in this inductively coupled RFID system [24].

These conditions are significantly different in the UHF band. A far-field region is used in UHF RFID systems and the radiated wave can be considered locally as a plane wave. In this region vectors of electric and magnetic field strength are perpendicular both to each other and to the direction in which the wave disperses. Since, the radiated electromagnetic wave of power density S is energy medium supplying transponders, the minimum power density S_{min} describes an EMF boundary condition that characterizes the IZ in UHF RFID system.

Despite the differences in the operation principles of HF and UHF RFID systems, the voltage induced in the transponder antenna when it is in the EMF of RWD antenna can be represented by the source U_{RT} in the generalized model. The electromagnetic induction phenomenon determines energy transmission without any galvanic connections and is represented by the voltage U_T that is induced at terminals of the connected antenna as well as by the power P_T received in the transponder. The electronic chip is designed to be supplied by the minimal voltage U_{Tmin} (HF band) or the minimal power P_{Tmin} (chip sensitivity in the UHF band) which are enough for activating internal circuits of the transponder that is located at the IZ boundary. The U_{Tmin} and P_{Tmin} parameters are used to determine characteristic values of the chip impedance (Z_{TC} boundary conditions: C_{TC} for the $f_0 = 13.56$ MHz [25], $Z_{TC}(P_{Tmin})$ for the $f_0 = 860$ – 960 MHz [26]) that are the first criterion in the antenna designing process.

In the HF RFID systems, the transponder antenna is made in a form of a rectangle [9], a square [10], a circle [11] or another polygon loop [19], which is small in relation to the wavelength λ (because λ is about 22 m). The impedance matching is obtained for the parallel resonance between the inductance L_{TA} and the capacitance C_{TC} of an active chip. Besides L_{TA} inductance and R_{TA} resistance (for the carrier frequency $f_0 = 13.56$ MHz), the database of parameters designated to antenna of RFID transponder operating in the HF band should be completed with quality factor Q_{TA} :

$$Q_{TA} = \frac{\omega L_{TA}}{R_{TA}} \quad (3)$$

In RFID systems of the UHF band, the transponder antennas are made in different shapes and technologies [12–19] and their sizes are always matched to the wavelength. Furthermore, the full impedance matching of antenna and chip is obtained when $Z_{TA} = Z_{TC}^*$ at the chip sensitivity P_{Tmin} (where * indicates the complex conjugate). The quality of this matching is defined on the basis of the power transfer coefficient τ which is defined as follows:

$$\tau = \frac{4\text{Re}(Z_{TA})\text{Re}(Z_{TC})}{\text{Re}(Z_{TA} + Z_{TC})^2 + \text{Im}(Z_{TA} + Z_{TC})^2} \quad (4)$$

The database of impedance parameters for the RFID transponder antennas operating in the UHF band consists of real and imaginary part of the Z_{TA} impedance that is determined for the frequency $f_0 = 860$ – 960 MHz (depending on world regions).

In both frequency bands, application conditions of RFID systems are the second key determinant for designing antennas – there is no universal RFID transponder, which could be used to mark any objects. Such a transponder should be designed for an object, in view of many conditions of its performance in the RFID system.

3 Validation of Impedance Parameters

3.1 Algorithm

The algorithm (Fig. 2) that is dedicated to validate the impedance parameters of transponder antenna operating in the HF or UHF band is elaborated on the basis of the model presented in Sect. 2. It consists of four steps carried out successively: (1) antenna designing, (2) its manufacturing, (3) measuring of the specified impedance parameters and (4) the parameter experimental verification. The determinants described in the model (Z_{TC} boundary and application conditions of RFID system) are the input data for the first and fourth stage of the algorithm.

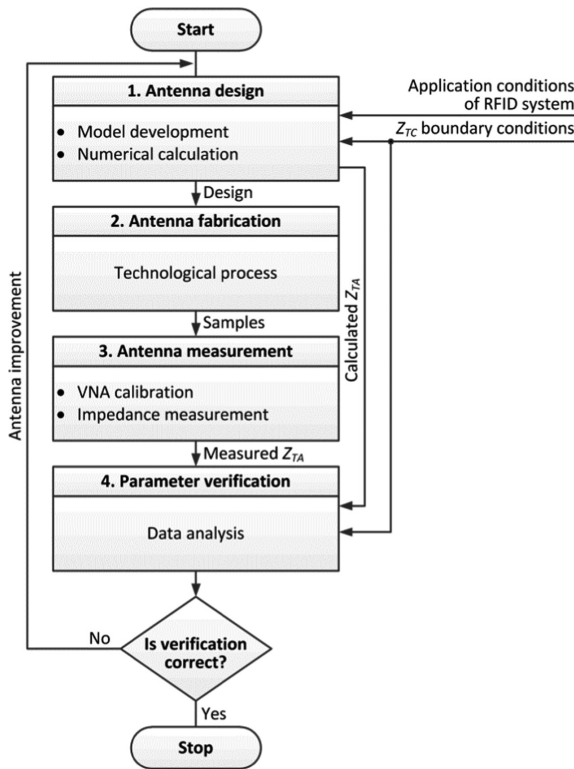


Fig. 2. Algorithm of proposed validation process

It should be noted that the stages of the antenna design/fabrication and the parameter verification have to be carried out by using advanced know-how, software and technological processes that are available in a R&D laboratory. It involves designers' key abilities essential for method implementation such as the selection of suitable apparatus, the calibration of the used equipment as well as the art of measuring impedance parameters of RFID transponder antennas by using sophisticated devices.

3.2 Antenna Measurement

Model. Methods and procedures that are commonly used for 50/75 Ω antennas operating in typical radio communications systems (such as: TV, GSM, UMTS, LTE, WiFi and many others) cannot be used for measuring parameters of HF or UHF RFID transponders. It is primarily due to the discussed phenomenon of untypical matching of impedance Z_{TA} and Z_{TC} (at the Z_{TC} boundary conditions), and also balanced HF [9–11] and UHF [12–18] antenna designs. Therefore the suitable test procedure for the antenna under test (AUT) consists in realization of indirect differential measurements of impedance parameters by using two 50 Ω coaxial ports (P1, P2) of a vector network analyzer (VNA) [27, 28] and a dedicated passive differential probe (PDP) with the S-S (signal to signal) contact tips [23].

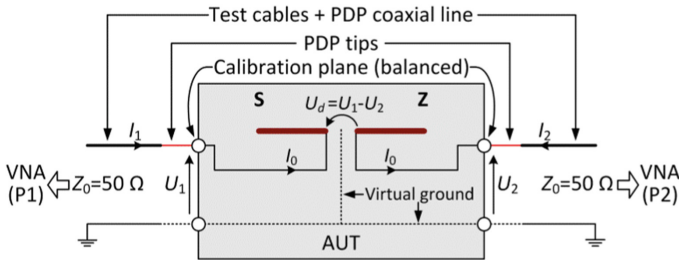


Fig. 3. Network model for AUT measurement

The measuring process can be described by the model (Fig. 3) in which a typical linear 2-port network is characterized by the impedance or scattering matrix (denoted as: Z , S). The S -parameters measurements does not provide the impedance (1) reading directly from the testing device. Hence it is necessary to determine the differential impedance Z_d and since the AUT current $I_0 = I_1 = -I_2$, it can be calculated from the following dependence:

$$Z_d = \frac{U_d}{I_0} = \frac{U_1 - U_2}{I_0} \tag{5}$$

where:

$$\begin{cases} U_1 = I_0 Z_{11} - I_0 Z_{12} \\ U_2 = I_0 Z_{21} - I_0 Z_{22} \end{cases} \quad (6)$$

On the basis of (5) and (6), the Z_d depends only on impedance parameters of the modeled network:

$$Z_d = Z_{11} - Z_{12} - Z_{21} + Z_{22} \quad (7)$$

The direct relation between \mathbf{Z} and \mathbf{S} matrix is given by [23].

$$\mathbf{Z} = \mathbf{Z}_0(\mathbf{1} - \mathbf{S})^{-1}(\mathbf{1} + \mathbf{S}) \quad (8)$$

where: the system reference impedance Z_0 is 50Ω and $\mathbf{1}$ denotes the unit matrix.

On the basis of (7) and (8), the differential impedance Z_d is finally given as follows:

$$Z_d = \frac{2Z_0(S_{12}S_{21} - S_{11}S_{22} - S_{12} - S_{21} + 1)}{(1 - S_{11})(1 - S_{22}) - S_{12}S_{21}} \quad (9)$$

Measurement Setup. In relation to the proposed network model, the two coaxial 50Ω line (VNA/probe test cables, PDP) have to be used in the measurement procedure (Fig. 4).

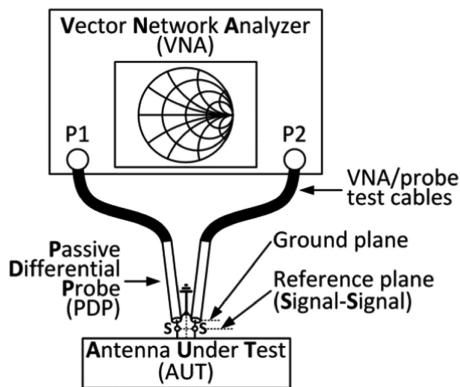


Fig. 4. Block diagram of measurement setup

The AUT should be matched to the chip impedance Z_{TC} . The typical value of chip resistance $\text{Re}(Z_{TC})$ equals from a few to tens of Ω for the chip sensitivity P_{Tmin} . The value of chip reactance $\text{Im}(Z_{TC})$ that is equal typically a few hundred ohms depends mostly on an internal capacitance that accumulates energy necessary for supplying the circuitry of transponder [26]. Therefore thin semi-rigid coaxial cables that extend tips to at least several mm should be used in the impedance measurements of the balanced

antenna. Such a PDP construction constitutes an acceptable compromise which concerns the probe casing impact on impedance measurements and also possibility of reaching the VNA calibration in the reference plane [23, 29, 30].

Calibration Procedure. In most similar cases, the calibration procedure is performed by using open/short port extension methods [15, 17, 29, 30]. It is used to shift the calibration plane to the tips of the PDP. In the first step, standard calibration is conducted at the end of the VNA/probe test cables. Next, the port extension technique (typically open method) is used to shift the calibration plane to probe tips (reference plane). It should be emphasized, that the discrepancies between measuring paths of the PDP significantly influences the accuracy of S parameter measurements and hence the value of the differential impedance Z_d (9). Moreover, the port extension is a less accurate correction of the VNA [31], because it does not remove mismatch effects induced by adding the PDP.

Higher accuracy of conducted measurements can be achieved by attempting to calibrate the both paths of the VNA by using specialized calibration standards that are implemented in the PDP [17, 23]. In this case, the calibration process involves also the PDP characterization as well as using the embed/de-embed features [32]. The problem is, however, that the PDP has no output terminal of ground and also both coaxial lines of this probe are permanently connected to each other. The calibration with the use of prepared short-open-load (SOL) elements that are soldered at the ends of the P1 and P2 lines [17], is not very accurate and leads to destruction of PDPs. On the other hand, it is possible to design a model of the probe in the specialized software [33] but it is time-consuming and often unattainable (e.g. the probe parameters cannot be found in the producers' specifications, the experimental verification of the model is impossible). Bearing in mind the mentioned problems, calibration substrates with short, open, load and thru (SOLT) standards [34, 35] that are usually dedicated for S -parameter calibrations and time-domain reflectometry (TDR) impedance validations are used in the procedure proposed by the authors of the paper. This method does not influence the destruction of PDPs.

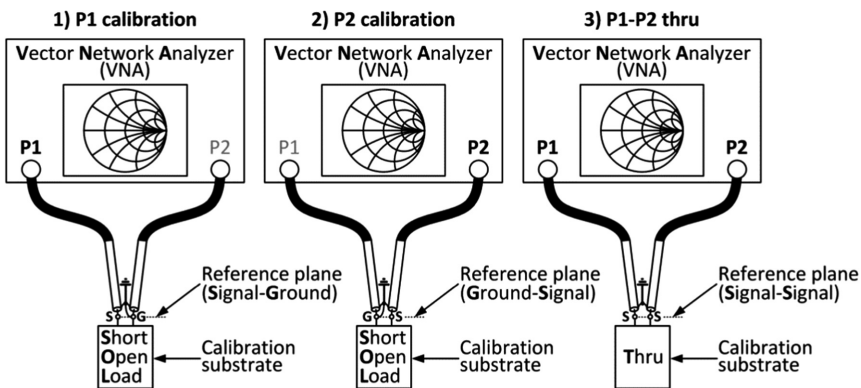


Fig. 5. Block diagram of proposed calibration procedure

In the proposed method, the configuration SG (Signal-Ground) for the P1 calibration and GS (Ground-Signal) for the P2 calibration is alternately created for the PDP (Fig. 5). These configurations are realized by shorting one of the probe tips to the ground. This converts the PDP into a 50Ω probe. In the first step, the tip of the P2 probe is shorted and then the SOL calibration for P1 is conducted. In the second step, the similar calibration is performed for P2 at the shorted tip of P1 probe. In the third step, the thru calibration is realized for SS (Signal-Signal) connection established between tips of the probes. In effect, this procedure allows to perform calibration and to move the measurement reference point to the PDP tips. The proposed method of removing the PDP errors can be supported by various calibration substrates and VNAs. The details of the method and an example of calibration are presented in Sect. 4.2. After calibration, the S scattering matrix is measured and results are used in the impedance calculations on the basis of (9) and (1) equations. These parameters are necessary for designing efficient antennas.

4 Results

4.1 Measurement Setup

The practical usefulness of the developed method has been presented on the basis of two representative examples, successively for the considered HF and UHF frequency bands. The measurement process has been done by using the test stand prepared in the RFID laboratory at the DETS RUT (Fig. 6).

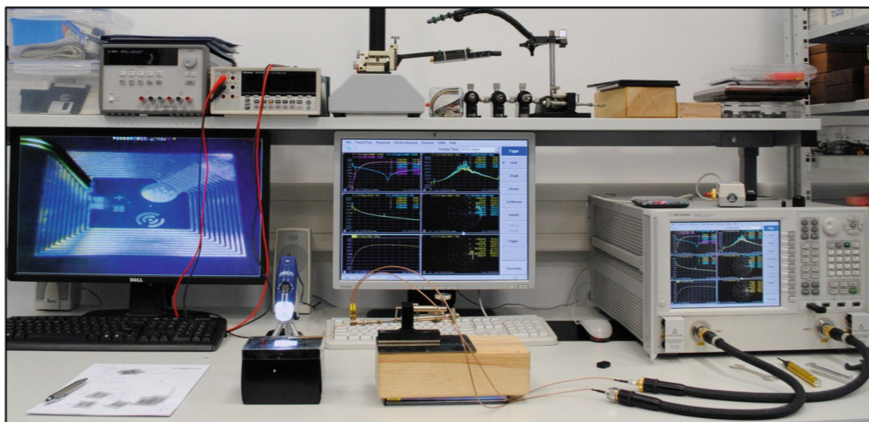


Fig. 6. Test stand – example for HF band

The S -parameters of AUT were measured by using the VNA Keysight PNA-X N5242A and commercially available probe (Micromanipulator 44-8000-D-NA) [36]. In the test stand, the probe is mounted on an economical manipulator (Micromanipulator model 110) which is feature with 3-axis direct leadscrew-leadnut drives (resolution $2.2 \mu\text{m}$, 10 mm max travel each axis) [36]. The analyzer and probe are connected by: the Keysight 85131F flexible cable set 3.5 mm (VNA test ports) to

3.5 mm (PDP cables), and the manually prepared RG178 UMC (probe connectors) to SMA (VNA flexible cable set).

4.2 Calibration

The test stand was calibrated at the probe tips by using the PacketMicro TCS50 substrate (Fig. 7). This calibration substrate is produced on the polished alumina (size: $17.3 \times 9.4 \times 0.6$ mm). It contains open, short, thru, 50Ω , and 100Ω gold contacts (accuracy: $<0.5\%$ for the 50Ω) with GS/SG configuration and probe pitches from 0.2 mm to 1.5 mm [35]. The size of contacts and pitch of the selected probe and calibration substrate is compatible with the typical lead spacing of RFID chips dedicated to the HF as well as UHF bands and provided in various types of packages.

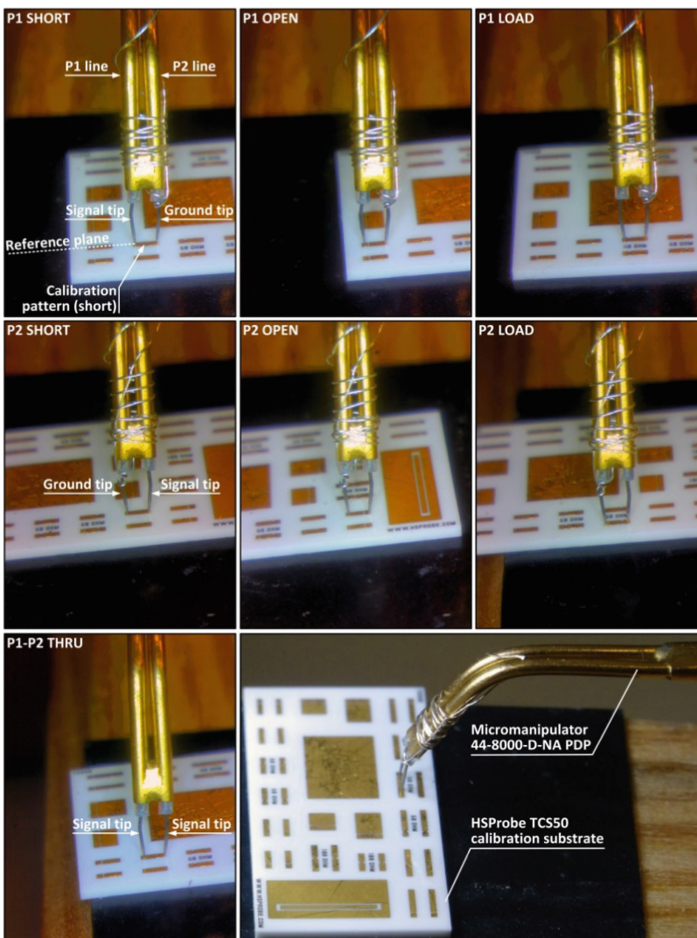


Fig. 7. PDP calibration

The calibration procedure on the laboratory stand is conducted in three steps (Fig. 7) that are discussed in details in Sect. 3.2. In order to meet the requirements assumed for the test stand, the calibration is made in the frequency band from 10 MHz

to 4 GHz (Fig. 8). The configurations SG for P1 and GS for P2 are prepared with using a thin silver plated wire. The shorting between selected signal and ground is realized by wrapping the wire around one of the probe tips and then around the PDP body.

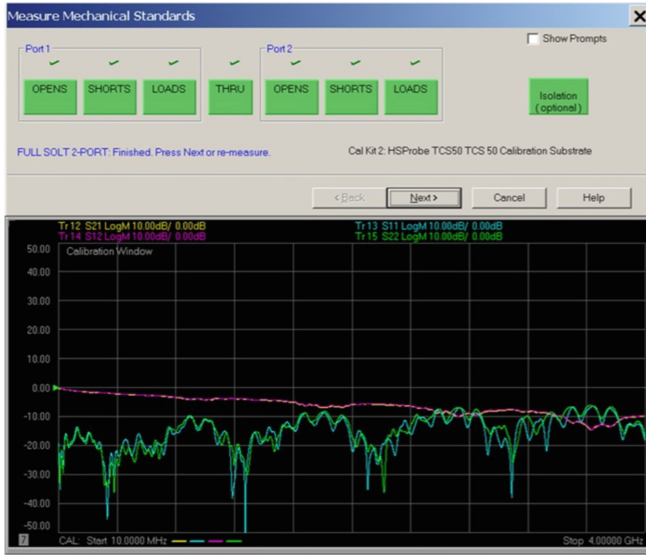


Fig. 8. Full SOLT 2-port calibration results

After this procedure, the P1–P2 thru configuration is represented only as a dot on the Smith chart (Fig. 9). It means that the reference plane is moved to the probe tips. Therefore the VNA calibration allows accurate and repetitive measurements of the differential impedance (9) in the test stand.

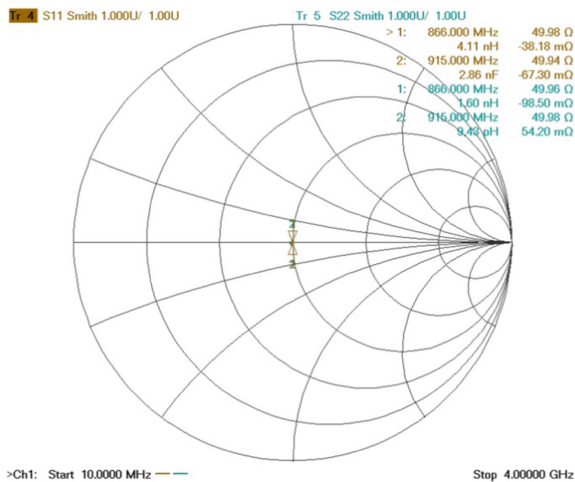


Fig. 9. Smith chart with P1–P2 thru

4.3 Example of HF Transponder Antenna

The stages: “3. Antenna measurement” and “4. Parameter verification” (Fig. 2) are discussed on the basis of two practical examples. The numerical results are compared with data obtained during measurements. The antennas have been designed and simulated by using Mentor Graphics HyperLynx 3D EM (HL3DEM) software.

The antenna of HF transponder designed for Talkin Things Company is analyzed as the first example. It is in the shape of a square of size 19×19 mm and is presented in Fig. 10. The impedance matching is provided for the chip NXP NT2H1001, NTAG 210 μ in FFC bump package. This chip complies with the requirements of the following communication protocol: ISO/IEC 14443 Type A, NFC Forum Type 2 ($C_{TC} = 50$ pF) [37]. The numerical model of the antenna has been elaborated in HL3DEM software tool, in the RFID laboratory at the DETS RUT. The test samples of inlays have been manufactured by selected supplier in China.

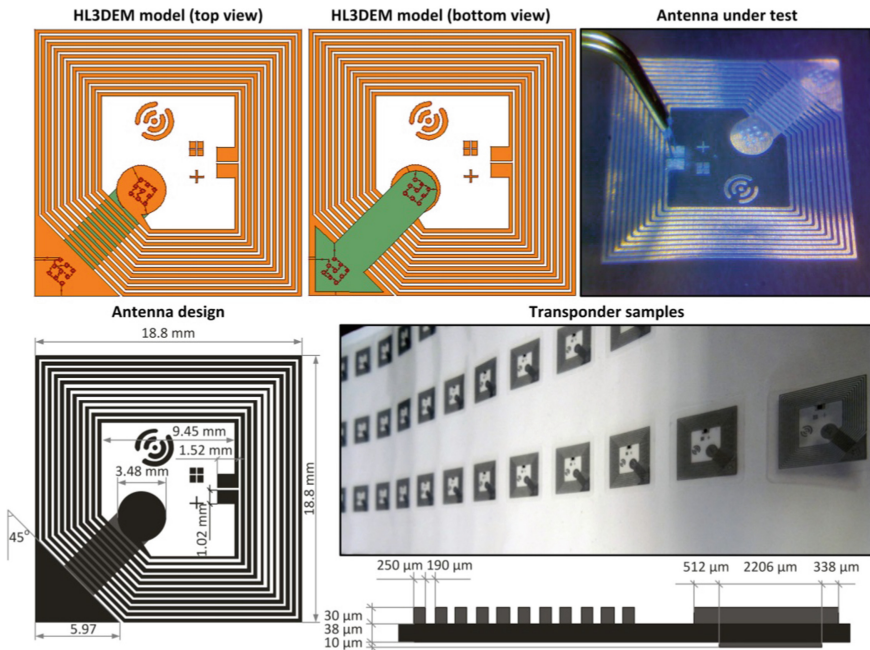


Fig. 10. Talkin Things 19×19 mm HF transponder

The model consists of two layers: the upper layer with RFID chip and windings of antenna, and the bottom one with bypass trace of the inductive loop. Moreover, real localization of vias, metal logotype of the company owner and contact pads to which the chip is attached are implemented in the model in order to gain the accuracy of the calculations. The PET film (thickness $38 \mu\text{m}$, dielectric constant $\epsilon_r = 3.4$ and loss $\text{tg}\delta = 0.0026$) is considered as a substrate for the modeled antennas.

Constant width of traces (0.25 mm) and trace to trace spacing (0.19 mm) are given into the antenna loop design. The thicknesses of the upper and bottom conductive

layers are assumed to be equal to 30 μm and 10 μm respectively. Due to the lack of detailed information about the technological process defined as aluminum etching, the typical conductivity value ($\sigma = 3.5 \cdot 10^7$ S/m) of such material is assumed in the calculations.

The basic antenna impedance parameters for the given type of the RFID transponders have been calculated with using the prepared numerical model. They have been determined for the carrier frequency $f_0 = 13.56$ MHz. Obtained results are compared with the measurement data that are averaged for 11 gathered samples (Table 1).

Table 1. Calculated and measured parameters of HF transponder antenna

Parameter	HL3DEM calculation results	Measurement results ^a
L_{TA} , μH	2.56	2.55 ± 0.01
R_{TA} , Ω	4.32	5.11 ± 0.61
Q_{TA} , -	50.49	42.52 ± 5.09

^aAverage of 11 samples and expanded uncertainty for a coverage factor $k = 2.28$ and a level of confidence $p \cong 95\%$

The measured average value of the inductance L_{TA} is convergent with the calculations obtained on the basis of the numerical model. The reported inaccuracy of the quality factor is caused by the different values established for the resistance R_{TA} . It is due to the lack of information about the real conductivity of the metal that is used in the technological process of manufacturing the tested antennas. It is suggested that the purity of aluminum alloy that is used to form metal layers in the measured samples is slightly smaller than it is assumed in the model (than $\sigma < 3.5 \cdot 10^7$ S/m).

4.4 Example of UHF Transponder Antenna

The second example concerns an antenna design for a semi-passive RFID sensor transponder operating in the UHF band (Fig. 11). The demonstrator of the circuit has been elaborated in the research/development project under the title “The development of zero-energy quantum system with active packets complex” (POIR.01.01.01-00-0407/16) realized for an industry partner (Aluron) and financed by the government (NCBR). The impedance matching in the design is provided for the chip AMS SL900A in QFN16 package [38] for which the dependence $Z_{TC}(P_{Tmin})$ at $f_0 = 860\text{--}960$ MHz is known [26]. The SL900A is an EPC global Class 3 transponder chip which is fully EPC Class 1 compliant (standardized by the ISO/IEC 18000-63) with additional custom commands for extended functions (RFID sensor transponder).

As previously, the numerical model of the antenna has been elaborated in HL3DEM software tool, in the RFID laboratory but the measuring samples of the demonstrator have been manufactured in the laboratory of integrated electronic micro- and nanotechnology HYBRID at the DETS RUT. The process of cutting out metal layers has been realized by using PCB plotter LPKF ProtoMat S100. The modeled elements of the transponder and its antenna are designed on selected epoxy laminate

which is suitable for advanced RF applications (ISOLA FR408: substrate thickness 0.51 mm, copper thickness 35 μm , dielectric constant $\epsilon_r= 4.19$, loss tangent $\text{tg}\delta = 0.0102$ for $f = 1 \text{ GHz}$) [39].

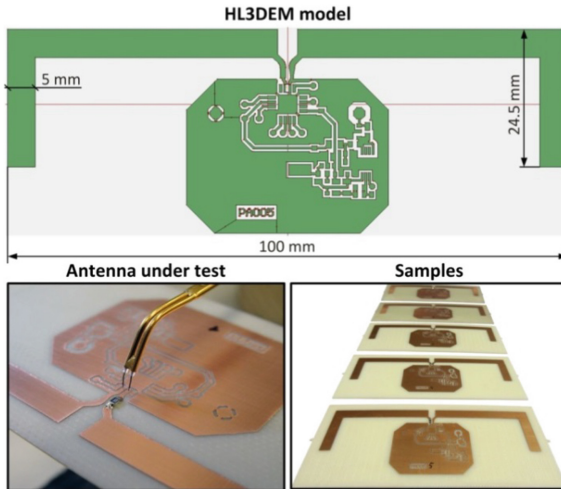


Fig. 11. UHF transponder

The basic antenna impedance parameters for the given type of the RFID transponders have been calculated with using the prepared numerical model. They have been determined in the frequency band 800–1000 MHz. Obtained results are compared with the measurement data that are averaged for 5 gathered samples (Fig. 12).

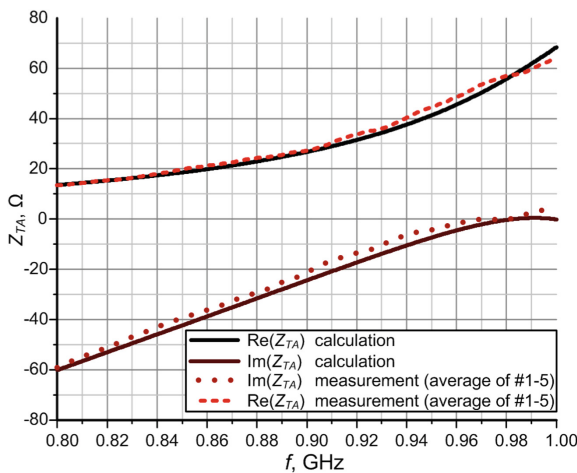


Fig. 12. Calculated and measured parameters of UHF transponder antenna

In this case, the obtained results of the impedance Z_{TA} show a satisfactory convergence (Pearson correlation coefficient is equal 0.938 for real part and 0.995 for imaginary part of impedance Z_{TA}) suitable for analyzing the impedance matching between antenna and selected chip in the whole RFID UHF band (860–960 MHz).

5 Conclusion

At the beginning it should be emphasized that there is no universal RFID transponder which could be used to mark any objects and to work in any standard of the radio frequency identification. Every transponder should be specially designed for an object, in view of many conditions of its performance in the RFID system. Moreover all steps of creating new efficient RFID devices involve using advanced know-how, software tools and technological processes that are available only in R&D laboratories. But designers' abilities (such as selection of suitable apparatus, the calibration of the used equipment, the art of measuring parameters in the time and frequency domain) are the most important for implementing successively research and development procedures in the considered scope.

Since the test methods that are commonly used for 50/75 Ω antennas operating in typical radio communications systems cannot be used for determining parameters of HF or UHF RFID transponders, the authors have proposed algorithm consists in realization of indirect differential measurements of impedance parameters by using two 50 Ω coaxial ports P1 and P2 of a VNA and dedicated PDP with the S-S contact tips. In particular, the question of equipment calibration was taken into consideration in the paper. Bearing in mind the known problems of common methods, the solution that does not interfere in the PDP structure was revealed and the calibration substrates with short, open, load and thru standards that are usually dedicated for *S*-parameter calibrations and TDR impedance validations were used. After calibration, the **S** scattering matrix was measured and results were used in the calculations of the impedance that is necessary for designing efficient antennas.

The details of the method were explained on the basis of two representative examples, successively for the considered HF and UHF frequency bands. The measurement process was done by using the test stand prepared in the RFID laboratory at the DETS RUT and samples were prepared in cooperation with the authors' partners from the industry. The measurement results were compared with data obtained for numerical models in the Mentor Graphics HyperLynx 3D EM. Generally, the measured values were convergent with the calculations despite some discrepancies resulting from restricted information about parameters that are not revealed by producers.

Acknowledgments. Results of Grants No. PBS1/A3/3/2012 from Polish National Centre for Research and Development as well as Statutory Activity of Rzeszow University of Technology were applied in this work.

References

1. Plunkett, J.W.: *Plunkett's Telecommunications Industry Almanac 2018*, 2018th edn. Plunkett Research, Houston, USA (2017)
2. Ustundag, A., Cevikcan, E.: *Industry 4.0: managing the digital transformation*, 1st edn. Cham, Switzerland (2018)
3. Greengard, S.: *The Internet of Things*. The MIT Press, London, GB (2015)
4. IDTechEx: continued growth as market for RFID exceeds \$10bn milestone. *ID World Magazine*, 38–39, Dec 2015
5. Das, R., Harrop, P.: *RFID forecasts, players and opportunities 2014–2024*. Report, IDTechEx (2014)
6. Ustundag, A.: *The Value of RFID. Benefits vs. Costs*. Springer-Verlag, London (2013). <https://doi.org/10.1007/978-1-4471-4345-1>
7. Finkenzerler, K.: *RFID Handbook – Fundamentals and Applications in Contactless Smart Cards, Radio Frequency Identification and Near-Field Communication*, 3rd edn. Wiley (2010)
8. CEPT ERC: ERC recommendation 70-03, Relating to the use of Short Range Devices (SRD). Electronic Communications Committee (2017)
9. Fernández-Salmerón, J., Rivadeneira, A., Rodríguez, M.A.C., Capitan-Vallvey, L.F., Palma, A.J.: HF RFID tag as humidity sensor: two different approaches. *IEEE Sens. J.* **15**(10), 5726–5733 (2015). <https://doi.org/10.1109/JSEN.2015.2447031>
10. Jankowski-Mihulowicz, P., Kalita, W., Skoczylas, M., Węglarski, M.: Modelling and design of HF RFID passive transponders with additional energy harvester. *Int. J. Antennas Propag.*, 1–10 (2013). Article ID 242840. <https://doi.org/10.1155/2013/242840>
11. Saghlatoon, H., Mirzavand, R., Honari, M.M., Mousavi, P.: Investigation on passive booster for improving magnetic coupling of metal mounted proximity range HF RFIDs. *IEEE Trans. Microw. Theory Tech.* **65**(9), 3401–3408 (2017). <https://doi.org/10.1109/TMTT.2017.2676095>
12. Zamora, G., Zuffanelli, S., Aguila, P., Paredes, F., Martin, F., Bonache, J.: Broadband UHF-RFID passive tag based on split-ring resonator (SRR) and T-match network. *IEEE Antennas Wirel. Propag. Lett.* Accepted for publication (2018). <https://doi.org/10.1109/lawp.2018.2800166>
13. Jankowski-Mihulowicz, P., Kawalec, D., Węglarski, M.: Antenna design for semi-passive UHF RFID transponder with energy harvester. *Radioengineering* **24**(3), 722–728 (2015). <https://doi.org/10.13164/re.2015.0722>
14. Zamora, G., Zuffanelli, S., Paredes, F., Marti, F., Bonache, J.: Design and synthesis methodology for UHF-RFID tags based on the T-match network. *IEEE Trans. Microw. Theory Tech.* **61**(12), 4090–4098 (2013). <https://doi.org/10.1109/tmtt.2013.2287856>
15. Lu, Y., Basset, P., Laheurte, J.M.: Performance evaluation of a long-range RFID tag powered by a vibration energy harvester. *IEEE Antennas Wirel. Propag. Lett.* **16**, 1832–1835 (2017). <https://doi.org/10.1109/LAWP.2017.2682419>
16. Ramirez, R.A., Rojas-Nastrucci, E.A., Weller, T.M.: UHF RFID tags for On-/Off-metal applications fabricated using additive manufacturing. *IEEE Antennas Wirel. Propag. Lett.* **16**, 1635–1638 (2017). <https://doi.org/10.1109/LAWP.2017.2658599>
17. Zhang, Y.J., Wang, D., Tong, M.S.: An adjustable quarter-wavelength meandered dipole antenna with slotted ground for metallic and airily mounted RFID tag. *IEEE Trans. Antennas Propag.* **65**(6), 2890–2898 (2017). <https://doi.org/10.1109/TAP.2017.2690535>

18. Sohrab, A.P., Huang, Y., Hussein, M.N., Carter, P.: A hybrid UHF RFID tag robust to host material. *IEEE J. Radio Freq. Identif.* **1**(2), 163–169 (2017). <https://doi.org/10.1109/JRFID.2017.2765623>
19. Alibakhshi-Kenari, M., Naser-Moghadasi, M., Sadeghzadeh, R.A., Virdee, B.S., Limiti, E.: Dual-band RFID tag antenna based on the Hilbert-curve fractal for HF and UHF applications. *IET Circuits Devices Syst.* **10**(2), 140–146 (2016). <https://doi.org/10.1049/iet-cds.2015.0221>
20. Jankowski-Mihułowicz, P., Węglarski, M.: Definition, characteristics and determining parameters of antennas in terms of synthesizing the interrogation zone in RFID systems. In: Crepaldi, P.C., Pimenta T.C. (eds.) *Radio Frequency Identification*, Chapter 5, pp. 65–119. INTECH, Rijeka, Croatia (2017). <https://doi.org/10.5772/intechopen.71378>
21. Taoufik, S., Dherbécourt, P., El Oualkadi, A., Temcamani, F.: Reliability and failure analysis of UHF RFID passive tags under thermal storage. *IEEE Trans. Device Mater. Reliab.* **17**(3), 531–538 (2017). <https://doi.org/10.1109/TDMR.2017.2733519>
22. Bauernfeind, T., Renhart, W., Alotto, P., Bíró, O.: UHF RFID antenna impedance characterization: numerical simulation of interconnection effects on the antenna impedance. *IEEE Trans. Magn.* **53**(6), 1–4 (2017). <https://doi.org/10.1109/TMAG.2017.2655883>
23. Jankowski-Mihułowicz, P., Pitera, G., Węglarski, M.: The impedance measurement problem in antennas for RFID technique. *Metrol. Meas. Syst.* **21**(3), 509–520 (2014). <https://doi.org/10.2478/mms-2014-0043>
24. Jankowski-Mihułowicz, P.: Field conditions of interrogation zone in anticollision radio frequency identification systems with inductive coupling. In: Turcu, C. (eds.) *Radio Frequency Identification Fundamentals and Applications Bringing Research to Practice*, Chapter 1, pp. 1–26. INTECH, Rijeka, Croatia (2010)
25. Rizkalla, S., Prestros, R., Mecklenbräuker, C.F.: De-embedding transformer-based method for characterizing the chip of HF RFID cards. In: *IEEE Wireless Power Transfer Conference (WPTC)*, pp. 1–4, Taipei (2017). <https://doi.org/10.1109/wpt.2017.7953814>
26. Jankowski-Mihułowicz, P., Węglarski, M.: Determination of passive and semi-passive chip parameters required for synthesis of interrogation zone in UHF RFID systems. *Elektronika ir Elektrotechnika* **20**(9), 65–73 (2014). <https://doi.org/10.5755/j01.eee.20.9.5007>
27. Meys, R., Janssens, F.: Measuring the impedance of balanced antennas by an S-parameter method. *IEEE Antennas Propag. Mag.* **40**(6), 62–65 (1998). <https://doi.org/10.1109/74.739191>
28. Peruzzi, M., Masson, F., Mandolesi, P., Perotoni, M.: Technique for measurement of UHF RFID balanced antennas. *Electron. Lett.* **54**(2), 59–60 (2018). <https://doi.org/10.1049/el.2017.3989>
29. Qing, X., Goh, C.K., Chen, Z.N.: Impedance characterization of RFID tag antennas and application in tag co-design. *IEEE Trans. Microw. Theory Tech.* **57**(5), 1268–1274 (2009). <https://doi.org/10.1109/TMTT.2009.2017288>
30. Cai, C., Hong, W., Deng, L., Li, S.: Impedance measurement of RFID tag antenna based on different methods. In: *IEEE 5th International Symposium on Electromagnetic Compatibility*, pp. 1–4, Beijing (2017). <https://doi.org/10.1109/emc-b.2017.8260455>
31. Agilent Technologies: *Advanced Calibration Techniques for Vector Network Analyzers. Modern Measurement Techniques for Testing Advanced Military Communications and Radars*. 2nd edn. Agilent Technologies (2006)
32. Keysight Technologies: *De-Embedding and Embedding S-Parameter Networks Using a Vector Network Analyzer*. Application Note, 5980-2784EN, Keysight Technologies, USA (2017)

33. Wang, Q., Gao, Y., Fan, J., Drewniak, J., Zai, R.: Differential probe characterization. In: IEEE International Symposium on Electromagnetic Compatibility (EMC), pp. 780–785, Ottawa (2016). <https://doi.org/10.1109/isemc.2016.7571748>
34. Cascade Microtech: Probe Selection Guide – Impedance Standard Substrate (ISS). ProbeGuide-1017, Cascade Microtech (2017)
35. PacketMicro: TCS50 Calibration Substrate, S-Parameter Calibration and TDR Impedance Validation, Santa Clara, USA (2017)
36. Micromanipulator: Probe Tips and Probe Holders. Reference Manual, Carson City, Nevada, USA (2013)
37. NXP: NT2L1001_NT2H1001, NTAG 210 μ , NFC Forum Type 2 Tag compliant IC with 48 bytes user memory. Product data sheet, Rev. 3.0, 343930 (2016)
38. AMS: SL900A EPC Class 3 Sensory Tag Chip – For Automatic Data Logging. Datasheet, v1-07 (2016)
39. Jankowski-Mihułowicz, P., Lichoń, W., Pitera, G., Węglarski, M.: Determination of the material relative permittivity in the UHF band by using T and modified ring resonators. *Int. J. Electron. Telecommun.* **62**(2), 129–134 (2016). <https://doi.org/10.1515/eletel-2016-0017>